

Artificial intelligence in the detection of Radio Galaxies.

by Hanifa Teimourian

Dr., Physics Lecturer in the Faculty of Engineering, Near East University, Nicosia, Cyprus.

Abstract

The article deals with artificial intelligence and machine learning, applying two reference automatic learning algorithms: the decision tree and the backward propagation neural network implemented in 30% of the Galaxy data set to observe and analyze the classification performance of machine learning techniques. A sample of radio sources with a radio brightness of

1.4 GHz, $S_{1.4} > 10 \text{ mJy}$, which employs a new technique more efficient than previous methods, such as a pronounced spectral index or a small angular size, using near-infrared data to filter at low, they use radiogalaxies with redshift ($z < 2$) by including only sources with a very weak identification or no detection in the K band or $3.6 \mu\text{m}$.

INTRODUCTION.

Active Galactic Nuclei (AGN) are among the most luminous and energetic objects in the universe. Carl Seyfert [11] was the first to describe them as a class in 1943, but the physical processes occurring in these phenomena were first suggested by Woltjer [12], where it was noted the nuclei must be compact ($\sim 100 \text{ pc}$) and “extremely massive” ($> 10^8 M_{\odot}$).

Many theories tried to explain the extreme power of the AGN [13], but the common explanation today is that AGN must be powered by accretion onto super massive black holes [14]. AGN emission covers all wavebands, from X-ray through the optical and radio, while powerful AGN are very luminous and can be found at the highest redshifts. Another property of AGN is the high variability of their emission observed at all frequencies on short time scales, which can be explained by a very compact structure of the emission region.

DEVELOPMENT.

Radio galaxies.

Radio galaxies are radio loud AGN with luminosities up to 10^{39} W , they derive their energy from gravitational potential energy on galactic scales due to their central super massive black hole and their radio emission is due to the synchrotron emission. Their main

observed structural components are radio core, radio jets, radio lobes and hotspots. The radio core is located in the center of the host galaxy and associated with the nucleus. This component usually has a flat spectrum and a linear size of less than ~ 0.2 pc. Radio jets link the core to the outermost part of the radio structure and may be visible over all their path or just part of it. They are collimated by the magnetic fields and constitute a small part of the total radio flux density of the radio galaxy. Their spectral index is usually between

$$-0.8 < \alpha < -0.5, \text{ where we define } S_\nu \propto \nu^\alpha.$$

The lobes are double symmetrical structures located on either side of the nucleus and describe the extended region of radio emitting plasma. They also have steep radio spectra similar to the jets. Hotspots are bright components on the outermost part of the radio lobes with a linear size of ≤ 1 kpc. When the jet interacts with the intergalactic medium it can create a shock which converts part of the kinetic energy to relativistic particles which then emerge as hotspots.

A brief history of the Universe and the Epoch of Reionization.

The formation of the first galaxies played a crucial role in the evolution of structure in the universe but they also transformed the neutral intergalactic medium to ionised plasma, this period in the Universe is called the Epoch of Reionization. At redshift 1100 ($\sim 350,000$ years after the Big Bang) the density of the Universe has decreased and cooled enough to allow photons to decouple from baryons and make the universe transparent, and it is at this point that we are able to see the first radiation permeating throughout the Universe in the form of the cosmic microwave background (CMB) radiation. After this time, the universe entered the dark ages, where the first stars and galaxies had yet to form and there was essentially no source of high-energy photons in the Universe. After about 400 million years the first galaxies began to form and start to emit radiation [15]. This period marks the start of the Epoch of Reionization (EoR). At the beginning of the EoR, the intergalactic medium was predominantly neutral except the regions close to the first objects. After enough UV- radiation has been emitted from these first objects the temperature and ionised fraction of the gas increases until the neutral gas is reduced to a small fraction of the density of the Universe, allowing photons to traverse through the Universe without being absorbed by the neutral gas.

Some of the key aims of current and future facilities are to determine which sources are responsible for reionising the Universe, how quickly this occurred, and when it ended. To measure the speed at which reionization occurs, one needs to trace the evolution in the abundance of neutral hydrogen at these early epochs.

The first direct measurement that established that we are beginning to see the EoR at $z > 6$ came from observations of the highest-redshift quasars found by the SDSS [16-18]. They found evidence for a Gunn-Peterson trough [19], i.e. the complete absorption of Ly α photons resulting in a trough of zero flux shortward of the Ly α emission line in the high-redshift

quasars due to a high neutral fraction. From these observations it is now clear that the EoR was coming to an end around $z \sim 6.3$.

However, the Gunn-Peterson trough does not provide the complete picture. This is because neutral hydrogen is too good at absorbing Ly α photons, therefore information about the rate of evolution of the neutral fraction within the EoR is difficult to determine and relies on assumptions about the intrinsic line profile of the Ly α emission line in distant quasars [20].

An alternative method of tracing the neutral hydrogen abundance at these early epochs is to use the hyperfine transition of neutral hydrogen at a rest-frame wavelength of 21 cm, i.e. in the radio waveband. At $z > 6$ this line is redshifted to low frequencies ($\nu < 200$ MHz). It is only now becoming possible to observe these frequencies to sufficient depth where we may detect the signature of reionization through the 21 cm line with the imminent commissioning of the Low-Frequency Array and the Murchison Widefield Array [21], both of which lead towards the much larger Square Kilometre Array (SKA;[22]).

The evolution of neutral hydrogen within the EoR can be investigated broadly by two methods. The first utilizes the power spectrum variations in the intensity of the 21 cm radiation [24] and is where the majority of current work is concentrated. However, an alternative method would be to measure the 21 cm forest against background powerful radio sources [23], in much the same way that the Lyman- α forest is used to probe the intergalactic medium at lower redshifts. The key missing ingredient for this method to be successful is the discovery of powerful radio sources at sufficiently high redshift with which to observe the 21 cm forest.

High redshift radio galaxies.

High-redshift radio galaxies are powerful radio sources and hold the promise of being the ideal source with which to probe the evolution of Hi within the EoR. There have been many surveys which have tried to find high redshift radio galaxies [26-27-28-29-30], with the highest radio galaxy found thus far has a redshift of $z = 5.19$.

The problem that has hindered the discovery of more radio sources at the highest redshifts is not the paucity of deep radio data, but the difficulty of obtaining targeted follow-up spectroscopy of the many candidate sources within a given radio survey. This is due to the fact that powerful radio sources at z

> 5 radio sources make up $< 1\%$ of the total radio source population [35] in current large area radio

surveys such as the Faint Images of the Radio Sky at Twenty-centimetres (FIRST;[36]). To overcome this problem, previous studies have applied filtering criteria to eliminate lower redshift radio sources on the basis of their spectral index and/or angular size [26-28]. Indeed, this the selection of Ultra- Steep Spectrum radio sources resulted in the discovery of the highest redshift radio galaxy. However, it is clear that such methods are not 100 per cent efficient and a large number of radio sources at $z > 5$ may also be filtered out. This is crucially

important when the space density of the $z > 5$ radio source population is extremely low to start with.

Unlike QSOs, where the stellar emission is outshone by the emission from the accretion disk around the central supermassive black hole, radio galaxies also offer the opportunity to study the stellar populations of the most massive galaxies at the highest redshifts. Many studies have shown that powerful radio sources are Universally hosted by the most massive galaxies in the Universe at the epoch which they are observed [39-40], with many authors suggesting that they evolve into the brightest cluster galaxies in the low-redshift Universe [41-42]. Thus finding and studying the highest redshift radio sources not only enables the possibility of tracing the evolution of neutral hydrogen within the EoR but also allows us to investigate the speed at which the most massive galaxies form and the role of the central supermassive black hole in regulating the evolution of the host galaxy via AGN-driven feedback [43-44].

High redshift radio galaxies as probes of the EoR.

High redshift ($z > 2$) radio galaxies are a small subset of all radio sources. For the powerful nearby radio galaxy Cygnus A, at higher frequency the spectrum is steeper. If we assume that all powerful radio galaxies exhibit similar spectra, due to synchrotron or inverse Compton losses, we will see the steeper part of the spectra as the redshift increases. van Breugel & McCarthy (1990) showed that in the 3CR sample the spectral index and redshift ($\alpha - z$) correlation leads support to such a hypothesis.

Other surveys have also shown that radio sources with ultra-steep spectral index $\alpha > 1$ tend to be fainter and reside at higher redshift than the less steep spectral-index radio sources [26-34].

One physical interpretation of the $\alpha - z$ correlation is basically the relation between the band shifting and redshift, i.e. by increasing the redshift we could see the steeper part of the spectra. However, there is evidence that the spectra of at least some high-redshift radio sources are not curved, thus resulting in an absence of a steeper spectrum at high frequencies [45]. Another interpretation for the steeper radio spectra is needed and this could be that the high redshift radio galaxies reside in dense environments, as this is observed at low redshift. Since radio emission is more pressure confined in higher gas density environments, as a consequence radio lobe in rich galaxy clusters will expand adiabatically and lose energy via synchrotron and inverse Compton losses, resulting in a steeper radio spectra.

It is clear that methods such as steep-spectral index and angular size filtering are not 100 per cent efficient and a large number of radio sources at $z > 5$ may also be filtered out [34-39]. This is crucially important when the space density of the $z > 5$ radio source population is extremely low to start with

High redshift radio galaxy hosts.

These luminous radio galaxies have accreting super massive black holes, which emit at UV, optical, and soft X-ray energies but the bulk of the UV and optical emission is absorbed by dust, and allowing us a clear view of the host galaxy.

We have mentioned that the near infrared luminosity of high redshift radio galaxies makes them some of the most massive galaxies in the early universe, and the clumpy morphology of high redshift radio galaxies hosts is consistent with mergers and hierarchical models of galaxy evolution [46]. These distant sources may also be the progenitors of the most massive galaxies, brightest cluster galaxies and cD galaxies [41].

studies of high redshift radio galaxies have shown a tight correlation in the Hubble K -z diagram for powerful radio sources [39-47].

$$K(z) = 17.37 + 4.53 \log_{10} z - 0.31(\log_{10} z)^2.$$

The Radio Surveys.

Although near-infrared surveys reaching sufficient depth to eliminate low-redshift $z < 2$ radio galaxies now exist, appropriate radio data is still also required. However, different populations dominate radio surveys at difference flux-density limits and it is clear that in order to find high-redshift radio sources, in particular those that reside within the epoch of reionisation.

Faint images of the Radio Sky at twenty centimeters.

The Faint Images of the Radio Sky at Twenty Centimeters (FIRST) radio survey started in 1993 to produce the centimetre-wavelength equivalent of the Palomar observatory sky survey, which covers 10000 deg² of the sky. The observations were made in the B-configuration of the VLA and the data calibrated using the AIPS data reduction package which provides the angular resolution of 5'' and $\sigma_{\text{RMS}} \sim 0.13$ mJy. The FIRST catalogue is a good option for matching with optical surveys while the radio structures down to 5'' are resolved. In the catalogue, both peak and integrated flux density measurements are provided. They were measured by fitting a two-dimensional Gaussian to each intensity peak. The scientific properties of the FIRST survey are the following: good positional accuracy to have a large number of optical identification, the sensitivity to detect the radio sources below the break in the radio source counts ($\log N - \log S$) curve and angular resolution high enough to provide morphological classification of the sources.

Machine Learning Techniques; Models and Applications.

More than three decades, researchers and scientists have been emerging new techniques and methods on artificial intelligence in order to outperform the tasks that human beings are not capable. These tasks can be any problem from our daily lives. Even in last two decades, machine learning techniques with capabilities for classification, optimisation, and as well as prediction are developed for using to solve these problems. Many different and

challenging frameworks and models are proposed and available in the literature, and many interesting deployments have been increased in different fields such as physics, chemistry, computer communication networks, healthcare, and many more [1-2].

In this section, two machine learning algorithms; Back-propagation neural networks, and Decision Trees, which are considered in this research will be introduced, and discussed.

Back-propagation Neural Networks (BPNN).

Back-propagation neural network (BPNN) is the most common used and preferred artificial intelligence algorithm that is known as a supervised learning algorithm. In BPNN, it propagates back the error signal to update the weight during error minimisation. As mentioned, BPNN is popular because of its simplicity in implementation and efficiency in classification and prediction problems [1, 10–12, 21].

During the training phase of BPNN, error is calculated in output layer by comparing actual and target output and weights are updating according to the Equation 1.

$$w_j^{k+1} = w_j^k + lr(y_i - \hat{y}_i^k)x_{i,j} \quad (1)$$

where w_j^{k+1} and w_j^k are updated and old weights respectively, lr is learning rate parameter, y_i and \hat{y}_i^k are actual and target outputs respectively, and $x_{i,j}$ is the input instance.

Figure 1 shows general architecture of 3-layered BPNN.

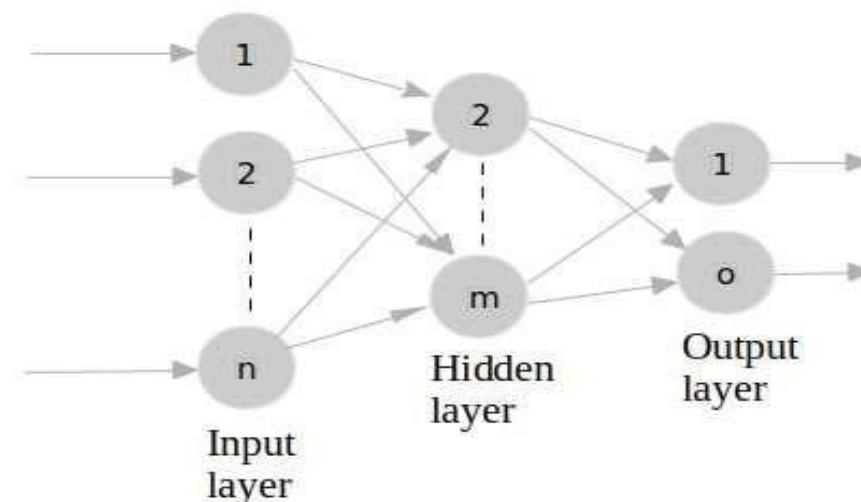


Fig. 1: General n-m-o architecture of BPNN.

Decision Tree (DT).

Another artificial intelligence method is decision trees (DT). DTs are tree-structured algorithms with initial root node, leaf nodes and decision nodes. In DTs, for classifying data, divide-and-conquer strategy is used until final leaf. Rules are assigned to each leaf and according to these rules, data flows until classified and decision trees have been used successfully in variety of classification problems recently [17–19].

For performing supervised classification, DT is a simple classifier in the form of a hierarchical tree structure. It comprises a directed branching structure with a series of questions. Simplicity and the speed are the main advantages of decision trees however, determination of initial root or the sequence of leaf nodes is the main drawback of decision trees. Figure 2 presents an example of a DT.

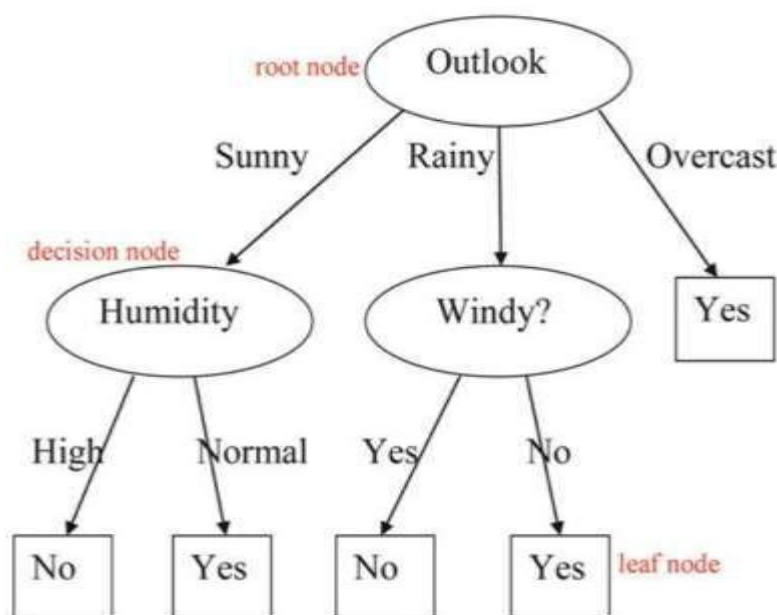


Fig. 2. Example decision tree.

Results and Discussions.

In this section, obtained results, discussions and comparisons will be presented. As stated earlier, the aim of this paper is to find the ideal classification algorithm considering achievement of optimal performance on Galaxy dataset. Thirty percent (30%) of instances of The Galaxy Dataset were considered that causes 30 patterns of total instances.

100 neurons were used in hidden layer of back-propagation neural network and Sigmoid activation function was used for hidden and output layers. 1000 epochs were used as stopping criteria of training for 70% training ratios.

For the experimental analysis, Decision Tree achieved 40% of classification ratio whereas Back Propagation Neural Networks achieved 73% classification ratio.

Table 1 shows all results obtained in this research and Figure 3 & 4 shows accuracy graphs for Back Propagation Neural Networks and Decision Tree Learning Algorithms respectively.

Table 1. Accuracy results for all methods.

Method	Accuracy
Decision Tree	40 %
Back-propagation NN	73 %

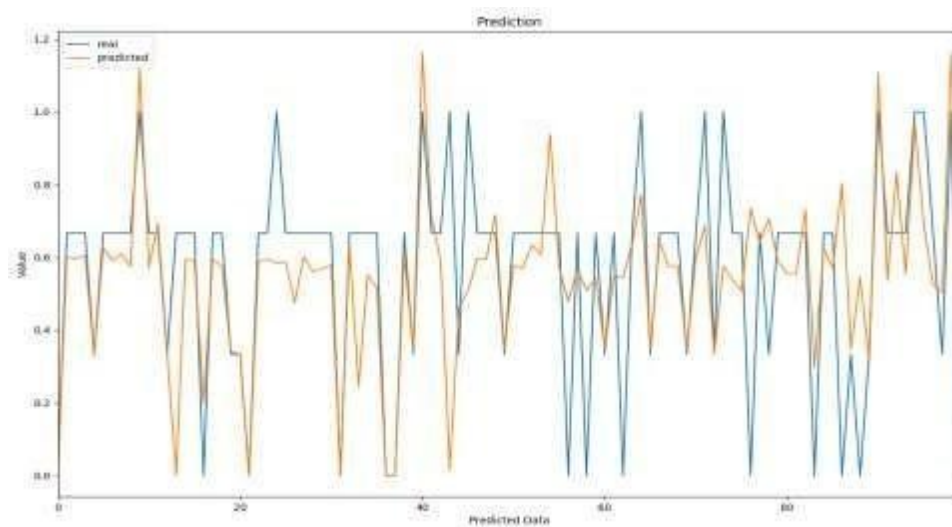


Fig. 3. BPNN Classification Graph.

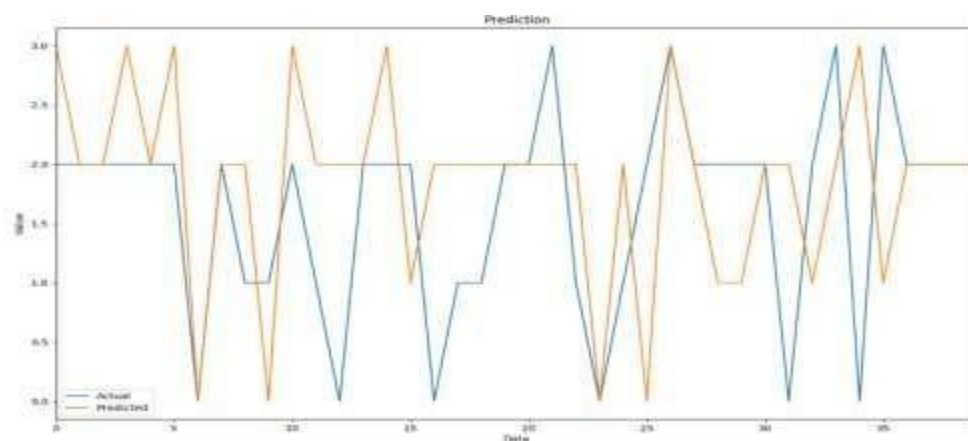


Fig. 4. DT Classification Graph

Considering above obtained results, Back-propagation neural network produced higher classification ratio with more steady results.

It is a general opinion in machine learning that the increment of training patterns or instances causes the increment of accuracy rates in classification results however, obtained results showed that either the efficiency of machine learning algorithms or the increment of the accuracy rates depend on the characteristics of dataset. In many two-class applications, Back-propagation Neural Networks produced superior results than Decision Trees in different studies. As it is mentioned above, those studies were performed for classification by different machine learning algorithms. These studies include different types of supervised or unsupervised neural network systems [2–3].

CONCLUSIONS.

Rapid developing of science and new technologies over the past decades have effected all aspects of human's life and so education. Dealing with extremely big data sets make teachers to apply computer science and artificial intelligence as part of their educational methods. Astronomy and astrophysics data sets evolution are among the fastest ones in science, thus the students are not training with traditional methods anymore.

In this paper, two benchmark machine learning algorithms; decision tree, and back-propagation neural network are implemented to 30% of The Galaxy Dataset in order to observe and analyze the classification performance of considered machine learning techniques. Obtained results show that machine learning techniques can efficiently classify the changes within the dataset and it can be concluded that the features of The Galaxy Dataset are linearly separable and do not need more complicated learning algorithms such as deep learning that increases computational time.

It is also obvious that more experiments with different parameters of considered machine learning techniques may increase accuracy rates. Future work will include the implementation of other machine learning algorithms such as Radial Basis Function Neural Network, Logistic Regression, and Random Forest by considering more data and make comparison between the learning methods as well as training ratio.

References.

1. Ever Y. K., Dimililer K., Sekeroglu B.: Comparison of Machine Learning Techniques for Prediction Problems, In: Barolli L., Takizawa M., Xhafa F., Enokido T. (eds). *Advances in Intelligent Systems and Computing (AISC)*. Web, Artificial Intelligence and Network Applications, WAINA 2019, 927, 1–11, Springer-Verlag Berlin Heidelberg, March 2019.
2. Ever, Y.K., Sekeroglu, B. and Dimililer, K., 2019, August. Classification Analysis of Intrusion Detection on NSL-KDD Using Machine Learning Algorithms. In *International*

Conference on Mobile Web and Intelligent Information Systems (pp. 111-122). Springer, Cham.

3. Sekeroglu B., Dimililer K. and Tuncal K., "Student Performance Prediction and Classification Using Machine Learning Algorithms" 8th International Conference on Educational and Information Technology (ICEIT 2019), Cambridge, UK, (2019).

4. Wu J., Chang C.: Classification of Landslide Features Using a LiDAR DEM and Back-Propagation Neural Network, In: H. M. El-Askary et al. (eds.). Advances in Remote Sensing and Geo Informatics Applications. Advances in Science, Technology & Innovation (ASTI), AG 2019, vol. 927, pp. 155–158, Springer-Verlag Berlin Heidelberg, (2019). 12

5. Chiba Z., Abghour N., Moussaid K., El omri A., Rida M.: A New Hybrid Framework Based on Improved Genetic Algorithm and Simulated Annealing Algorithm for Optimization of Network IDS Based on BP Neural Network, In: Ben Ahmed M., Boudhir A., Younes A. (eds) Innovations in Smart Cities Applications, 2nd edn.. Lecture Notes in Intelligent Transportation and Infrastructure, 507–521, vol 921. Springer, Cham, (2019).

6. Pal M. and Mather P.M., "Decision Tree Based Classification of Remotely Sensed Data", 22nd Asian Conference on Remote Sensing, Singapore, (2001).

7. Eissa M.M., Ali A.A., Abdel-Latif K.M. and Al-Kady A.F., "A frequency control technique based on decision tree concept by managing thermostatically controllable loads at smart grids", International Journal of Electrical Power and Energy Systems, Vol.108, 40-51, (2019).

8. Vernuccio F. Rosenberg M.D. Meyer M. Choudhury K.R., Nelson R.C. and Marin D., "Negative Biopsy of Focal Hepatic Lesions: Decision Tree Model for Patient Management", American Journal of Roentgenology, Vol.212 (3), (2019) 677-685.

9. Dougherty G.: Pattern recognition and classification: an introduction, Springer, Germany, (2012).

10. Ogidan E. T., Dimililer K., Ever Y. K.: Machine Learning for Expert Systems in Data Analysis, 2nd International Symposium on Multidisciplinary Studies and Innovative Technologies, ISMSIT2018, (2018).

11. Carl Seyfert.: No. 671. Nuclear emission in spiral nebula, Contributions from the Mount Wilson Observatory / Carnegie Institution of Washington, vol. 671, pp.1-13, (1943)

12. Kahn, F. D.; Woltjer, L.: Intergalactic Matter and the Galaxy, Astrophysical Journal, vol. 130, p.705, (1959).

13. Hoyle, F.; Fowler, William A.: Nature of Strong Radio Sources, Nature, Volume 197, Issue 4867, pp. 533-535, (1963).

14. Lynden-Bell, D.: Galactic Nuclei as Collapsed Old Quasars, Nature, Volume 223, Issue 5207, pp. 690-694, (1969).

15. Abel, Tom; Bryan, Greg L.; Norman, Michael L.: The Formation of the First Star in the Universe, Science, Volume 295, Issue 5552, pp. 93-98, (2002).

16. Fan, Xiaohui; Narayanan, Vijay K.; Lupton, Robert H.; Strauss, Michael A.; Knapp, Gillian R.; Becker, Robert H.; White, Richard L.; Pentericci, Laura; Leggett, S. K.; Haiman,

Zoltán; Gunn, James E.; Ivezić, Željko; Schneider, Donald P.; Anderson, Scott F.; Brinkmann, J.; Bahcall, Neta A.; Connolly, Andrew J.; Csabai, István; Doi, Mamoru; Fukugita, Masataka; Geballe, Tom; Grebel, Eva K.; Harbeck, Daniel; Hennessy, Gregory; Lamb, Don Q.; Miknaitis, Gajus; Munn, Jeffrey A.; Nichol, Robert; Okamura, Sadanori; Pier, Jeffrey R.; Prada, Francisco; Richards, Gordon T.; Szalay, Alex; York, Donald G.: A Survey of $z > 5.8$ Quasars in the Sloan Digital Sky Survey. I. Discovery of Three New Quasars and the Spatial Density of Luminous Quasars at $z \sim 6$, *The Astronomical Journal*, Volume 122, Issue 6, pp. 2833-2849, (2001)

17. Adelberger, Kurt L.; Steidel, Charles C.: Multiwavelength Observations of Dusty Star Formation at Low and High Redshift, *The Astrophysical Journal*, Volume 544, Issue 1, pp. 218-241., (2000)

18. Becker, Robert H.; Fan, Xiaohui; White, Richard L.; Strauss, Michael A.; Narayanan, Vijay K.; Lupton, Robert H.; Gunn, James E.; Annis, James; Bahcall, Neta A.; Brinkmann, J.; Connolly,

19. J.; Csabai, István; Czarapata, Paul C.; Doi, Mamoru; Heckman, Timothy M.; Hennessy, G. S.; Ivezić, Željko; Knapp, G. R.; Lamb, Don Q.; McKay, Timothy A.; Munn, Jeffrey A.; Nash, Thomas; Nichol, Robert; Pier, Jeffrey R.; Richards, Gordon T.; Schneider, Donald P.; Stoughton, Chris; Szalay, Alexander S.; Thakar, Aniruddha R.; York, D. G.: Evidence for Reionization at $z \sim 6$: Detection of a Gunn-Peterson Trough in a $z = 6.28$ Quasar, *The Astronomical Journal*, Volume 122, Issue 6, pp. 2850-2857, (2001).

20. Gunn, James E.; Peterson, Bruce A.: On the Density of Neutral Hydrogen in Intergalactic Space., *Astrophysical Journal*, vol. 142, p.1633-1636, (1965).

21. Mortlock, Daniel J.; Warren, Stephen J.; Venemans, Bram P.; Patel, Mitesh; Hewett, Paul C.; McMahon, Richard G.; Simpson, Chris; Theuns, Tom; Gonzáles-Solares, Eduardo A.; Adamson, Andy; Dye, Simon; Hambly, Nigel C.; Hirst, Paul; Irwin, Mike J.; Kuiper, Ernst; Lawrence, Andy; Röttgering, Huub J. A.: A luminous quasar at a redshift of $z = 7.085$, *Nature*, Volume 474, Issue 7353, pp. 616-619, (2011).

22. Williams, Christopher L.; Hewitt, Jacqueline N.; Levine, Alan M.; de Oliveira-Costa, Angelica; Bowman, Judd D.; Briggs, Frank H.; Gaensler, B. M.; Hernquist, Lars L.; Mitchell, Daniel A.; Morales, Miguel F.; Sethi, Shiv K.; Subrahmanyam, Ravi; Sadler, Elaine M.; Arcus, Wayne; Barnes, David G.; Bernardi, Gianni; Bunton, John D.; Cappallo, Roger C.; Crosse, Brian W.; Corey, Brian E.; Deshpande, Avinash; deSouza, Ludi; Emrich, David; Goeke, Robert F.; Greenhill, Lincoln J.; Hazelton, Bryna J.; Herne, David; Kaplan, David L.; Kasper, Justin C.; Kincaid, Barton B.; Koenig, Ronald; Kratzenberg, Eric; Lonsdale, Colin J.; Lynch, Mervyn J.; McWhirter, S. Russell; Morgan, Edward H.; Oberoi, Divya; Ord, Stephen M.; Pathikulangara, Joseph; Prabu, Thiagaraj; Remillard, Ronald A.; Rogers, Alan E. E.; Anish Roshni, D.; Salah, Joseph E.; Sault, Robert J.; Udaya Shankar, N.; Srivani, K. S.; Stevens, Jamie B.; Tingay, Steven J.; Wayth, Randall B.; Waterson, Mark; Webster, Rachel L.; Whitney, Alan R.; Williams, Andrew J.; Wyithe, J. Stuart B.: Low-frequency Imaging of Fields at High Galactic Latitude with the Murchison Widefield Array 32 Element Prototype, *The Astrophysical Journal*, Volume 755, Issue 1, article id. 47, 19 pp, (2012).

23. Carilli, C. L.; Rawlings, S.: Motivation, key science projects, standards and assumptions, *New Astronomy Reviews*, Volume 48, Issue 11-12, p. 979-984, (2004).
24. Carilli, C. L.; Gnedin, N. Y.; Owen, F.: H I 21 Centimeter Absorption beyond the Epoch of Reionization, *The Astrophysical Journal*, Volume 577, Issue 1, pp. 22-30, (2002)
25. Ilian T. Iliev, Garrelt Mellema, Ue-Li Pen, J. Richard Bond, Paul R. Shapiro.,: Current models of the observable consequences of cosmic reionization and their detectability, *Monthly Notices of the Royal Astronomical Society*, Volume 384, Issue 3, (2008)
26. Storrie-Lombardi, L. J.; McMahon, R. G.; Irwin, M. J.; Hazard, C.,: APM Z ≥ 4 QSO Survey: Spectra and Intervening Absorption Systems, *Astrophysical Journal* v.468, p.121, (1996)
27. De Breuck, C.; van Breugel, W.; Röttgering, H. J. A.; Miley, G.,: A sample of 669 ultra steep spectrum radio sources to find high redshift radio galaxies, *Astronomy and Astrophysics Supplement*, v.143, p.303-333, (200)
28. Röttgering, H. J. A.; Best, P. N.; De Breuck, C.; Kurk, J.; Pentericci, L.; van Breugel, W.,: Distant Radio Galaxies: the Present and Future, *ASTRON*. ISBN: 90-805434-1-1, 340 pages, 2000, p.65, (200)
29. De Breuck, C.; Downes, D.; Neri, R.; van Breugel, W.; Reuland, M.; Omont, A.; Ivison, R.,: Detection of two massive CO systems in 4C 41.17 at $z = 3.8$, *Astronomy and Astrophysics*, v.430, p.L1-L4, (2005)
30. Jarvis, M. J., van Breukelen, C., & Wilman, R. J.: The discovery of a type II quasar at $z = 1.65$ with integral-field spectroscopy, *Monthly Notices of the Royal Astronomical Society: Letters*, Volume 358, Issue 1, pp. L11-L15, (2005)
31. Matt J. Jarvis, Steve Rawlings, Mark Lacy, Katherine M. Blundell, Andrew J. Bunker, Steve Eales, Richard Saunders, Hyron Spinrad, Daniel Stern, Chris J. Willott,: A sample of 6C radio sources designed to find objects at redshift $z > 4$ - II. Spectrophotometry and emission-line properties, *Monthly Notices of the Royal Astronomical Society*, Volume 326, Issue 4, (2001)
32. Kauffmann, Guinevere; Heckman, Timothy M.; Tremonti, Christy; Brinchmann, Jarle; Charlot, Stéphane; White, Simon D. M.; Ridgway, Susan E.; Brinkmann, Jon; Fukugita, Masataka; Hall, Patrick B.; Ivezić, Željko; Richards, Gordon T.; Schneider, Donald P.,: the host galaxies of active galactic nuclei, *Monthly Notices of the Royal Astronomical Society*, Volume 346, Issue 4, pp. 1055-1077, (2003)
33. Dunlop, J. S.; Peacock, J. A.: The Redshift Cut-Off in the Luminosity Function of Radio Galaxies and Quasars, *Monthly Notices of the Royal Astronomical Society*, Vol. 247, NO. 1/NOV1, P. 19, (1990).
34. Kelle L. Cruz, I. Neill Reid, J. Davy Kirkpatrick, Adam J. Burgasser, James Liebert, Adam R. Solomon, Sarah J. Schmidt, Peter R. Allen, Suzanne L. Hawley, and Kevin R. Covey: Meeting the Cool Neighbors. IX. The Luminosity Function of M7-L8 Ultracool Dwarfs in the Field, *The Astronomical Journal*, Volume 133, Number 2, (2007)
35. Maria J. Cruz, Matt J. Jarvis, Katherine M. Blundell, Steve Rawlings, Steve Croft, Hans- Rainer Klöckner, Ross J. McLure, Chris Simpson, Thomas A. Targett, Chris J. Willott,: The

6C** sample of steep-spectrum radio sources – I. Radio data, near-infrared imaging and optical spectroscopy, *Monthly Notices of the Royal Astronomical Society*, Volume 373, Issue 4, (2006)

36. Wilman, R. J.; Miller, L.; Jarvis, M. J.; Mauch, T.; Levrier, F.; Abdalla, F. B.; Rawlings, S.; Klöckner, H.-R.; Obreschkow, D.; Olteanu, D.; Young, S.: A semi-empirical simulation of the extragalactic radio continuum sky for next generation radio telescopes, *Monthly Notices of the Royal Astronomical Society*, Volume 388, Issue 3, pp. 1335-1348, (2008)

37. Becker, Robert H.; White, Richard L.; Helfand, David J.: The FIRST Survey: Faint Images of the Radio Sky at Twenty Centimeters, *Astrophysical Journal* v.450, p.559, (1995)

38. Blundell, K. M., Rawlings, S., & Willott, C. J.: The Evolution of Classical Doubles: Clues from Complete Samples, *ASTRON*. ISBN: 90-805434-1-1, 340, (200)

39. Wil J. M. van Breugel, S. A. Stanford, Hyron Spinrad, Daniel Stern, and James R. Graham,: Morphological Evolution in High-Redshift Radio Galaxies and the Formation of Giant Elliptical Galaxies, *The Astrophysical Journal*, Volume 502, Number 2, (1998).

40. Jarvis, M. J., Rawlings, S., Willott, C. J., Blundell, K. M., Eales, S., & Lacy, M.: On the redshift cut-off for steep-spectrum radio sources, *Monthly Notices of the Royal Astronomical Society*, Volume 327, Issue 3, pp. 907-917, (2001)

41. Nick Seymour, Daniel Stern, Carlos De Breuck, Joel Vernet, Alessandro Rettura, Mark Dickinson, Arjun Dey, Peter Eisenhardt, Robert Fosbury, Mark Lacy, Pat McCarthy, George Miley, Brigitte Rocca-Volmerange, Huub Röttgering, S. Adam Stanford, Harry Teplitz, Wil van Breugel, and Andrew Zirm,: The Massive Hosts of Radio Galaxies across Cosmic Time, *The Astrophysical Journal Supplement Series*, Volume 171, Number 2, (2007)

42. R. J. McLure, M. J. Jarvis, T. A. Targett, J. S. Dunlop and P. N. Best: On the evolution of the black hole: spheroid mass ratio, *Mon. Not. R. Astron. Soc.* 368, 1395–1403, (2006)

43. Peter D. Herbert, Matt J. Jarvis, Chris J. Willott, Ross J. McLure, Ewan Mitchell, Steve Rawlings, Gary J. Hill and James S. Dunlop: The evolution of the Fundamental Plane of radio galaxies from $z \sim 0.5$ to the present day, *Mon. Not. R. Astron. Soc.* 410, 1360–1376, (2011)

44. Bower, R. G.; Benson, A. J.; Malbon, R.; Helly, J. C.; Frenk, C. S.; Baugh, C. M.; Cole, S.; Lacey, C. G.: Breaking the hierarchy of galaxy formation, *Monthly Notices of the Royal Astronomical Society*, Volume 370, Issue 2, pp. 645-655, (2006)

45. Croton, Darren J.; Springel, Volker; White, Simon D. M.; De Lucia, G.; Frenk, C. S.; Gao, L.; Jenkins, A.; Kauffmann, G.; Navarro, J. F.; Yoshida, N.: The many lives of active galactic nuclei: cooling flows, black holes and the luminosities and colours of galaxies, *Monthly Notices of the Royal Astronomical Society*, Volume 365, Issue 1, pp. 11-28, (2006)

46. I.J. Klammer, R.D. Ekers, J.J. Bryant, R.W. Hunstead, E.M. Sadler, C. De Breuck,: A search for distant radio galaxies from SUMSS and NVSS: III. radio spectral energy distributions and the z - α correlation, *Mon.Not.Roy.Astron.Soc.* 371:852-866, (2006).

47. Springel, Volker; White, Simon D. M.; Jenkins, Adrian; Frenk, Carlos S.; Yoshida, Naoki; Gao, Liang; Navarro, Julio; Thacker, Robert; Croton, Darren; Helly, John; Peacock, John A.; Cole, Shaun; Thomas, Peter; Couchman, Hugh; Evrard, August; Colberg, Jörg; Pearce,

Frazer,; Simulations of the formation, evolution and clustering of galaxies and quasars, *Nature*, Volume 435, Issue 7042, pp. 629-636, (2005)

48. Eales, S. A. & Rawlings, S.: A Panoramic View of Radio Galaxy Evolution from a Redshift of 0 to a Redshift of 4.3, *Astrophysical Journal* v.460, p.68, (1996)

49. Bryant, J. J.; Johnston, H. M.; Broderick, J. W.; Hunstead, R. W.; De Breuck, C.; Gaensler, B. M.: A new search for distant radio galaxies in the Southern hemisphere - III. Optical spectroscopy and analysis of the MRCR-SUMSS sample, *Monthly Notices of the Royal Astronomical Society*.

50. Chris J. Willott, Steve Rawlings, Matt J. Jarvis, Katherine M. Blundell: Near-infrared imaging and the K-z relation for radio galaxies in the 7C redshift survey, *Mon.Not.Roy.Astron.Soc.* 339 (2003) 173-188, (2002)

51. Lilly, S. J.: Discovery of a radio galaxy at a redshift of 3.395, *Astrophysical Journal*, Part 1 (ISSN 0004-637X), vol. 333, p. 161-167, (1988)

52. Sekeroglu B., Dimililer K., Tuncal, K., "Artificial Intelligence in Education: Application of Student Performance Evaluation", *Dilemas Contemporáneos: Educación, Política y Valores*. Año: VII, Número:1, Artículo no.:15, Período: 1 de Septiembre al 31 de diciembre, 2019.

[https://dilemascontemporaneoseducacionpoliticayvalores.com/_files/200005691-](https://dilemascontemporaneoseducacionpoliticayvalores.com/_files/200005691-641d6641d8/19.09.15%20La%20Inteligencia%20Artificial%20en%20Educaci%C3%B3n.pdf)

53. [641d6641d8/19.09.15%20La%20Inteligencia%20Artificial%20en%20Educaci%C3%B3n.pdf](https://dilemascontemporaneoseducacionpoliticayvalores.com/_files/200005691-641d6641d8/19.09.15%20La%20Inteligencia%20Artificial%20en%20Educaci%C3%B3n.pdf)

54. Amirjanov A., Dimililer K., "Image compression system with an optimization of compression ratio", *IET Image Processing*. Accepted: June 2019, Published: July 2019. DOI: 10.1049/iet-ipr.2019.0114, Print ISSN: 1751-9659.

55. Dimililer K., Mekonnen G. A., "Optical Mark Reader System (OMRS) using Web Based Image Scanners", *Dilemas Contemporáneos: Educación, Política y Valores*. Año: VI Número: Edición Especial Artículo no.:34 Período: Julio, 2019. [https://dilemascontemporaneoseducacionpoliticayvalores.com/_files/200005364-](https://dilemascontemporaneoseducacionpoliticayvalores.com/_files/200005364-8a0e58b095/EE%2019.07.34%20Sistema%20de%20Lector%20%C3%93ptico%20de%20Marcas.pdf)

56. [8a0e58b095/EE%2019.07.34%20Sistema%20de%20Lector%20%C3%93ptico%20de%20Marcas.pdf](https://dilemascontemporaneoseducacionpoliticayvalores.com/_files/200005364-8a0e58b095/EE%2019.07.34%20Sistema%20de%20Lector%20%C3%93ptico%20de%20Marcas.pdf)

57. Ever Y. K., Dimililer K., "The effectiveness of a new classification system in higher education as a new e-learning tool ", *Quality & Quantity*, Springer-Verlag, Vol. 52, Issue 1, pp. 573-582, Accepted: 2017, published: December 2018. DOI: 10.1007/s11135-017-0636-y.

58. Dimililer K., "Use of Intelligent Student Mood Classification System (ISMCS) to achieve high quality in education", *Quality & Quantity*, Springer-Verlag, Vol. 52, Issue 1, pp. 651-662, Accepted: 2017, published: December 2018. DOI: 10.1007/s11135-017-0644-y.